70th International Astronautical Congress, October 21–25, 2019, Washington, D.C., United States.

IAC-19.D2.5.3

Architectures of Hybrid Navigation Systems (HNS) for Reusable Space Transportation Systems

René Schwarz[1⋆†], **Marco Solari**[2†], **Bronislovas Razgus**[3†], **Matias Bestard Körner**[4†], **Benjamin Braun**[5‡], **Michael Dumke**[6†], **Markus Markgraf**[7‡], **Martín Reigenborn**[8†], **Jan Sommer**[9§], **Dennis Pfau**[10§], **Thomas Thiele**[11¶], **Johannes Riehmer**[12¶]

[†] German Aerospace Center (DLR), Institute of Space Systems
Robert-Hooke-Str. 7, DE–28359 Bremen, Germany

[‡] German Aerospace Center (DLR), Space Operations and Astronaut Training
Oberpfaffenhofen, DE–82234 Weßling, Germany

[§] German Aerospace Center (DLR), Simulation and Software Technology
Lilienthalplatz 7, DE–38108 Braunschweig, Germany

[¶] German Aerospace Center (DLR), Institute of Aerodynamics and Flow Technology
Dept. of Supersonic and Hypersonic Technology, Linder Höhe, DE–51147 Köln, Germany

[⋆] Corresponding author

Abstract

This paper outlines the development of two Hybrid Navigation Systems (HNS) for recent Vertical Takeoff, Horizontal Landing (VTHL) and Vertical Takeoff, Vertical Landing (VTVL) Reusable Launch Vehicle (RLV) missions and describes the challenges faced for the development of navigation systems for such applications. It provides an overview of the principal HNS architecture, which is commonly developed for both missions, and presents the selected sensor suites with Global Navigation Satellite System (GNSS) receivers, Differential GNSS (DGNSS), Sun sensors, laser and radar altimeters, and Flush Airdata Sensing (FADS) systems as non-inertial sensors including the required ground-based means and infrastructure. It concludes with a preliminary assessment of the achievable navigation performance for each of these missions.

Keywords: Hybrid Navigation; Navigation Systems; GNC; Sensors; Reusable Launch Vehicles; Flight Experiments

Abbreviations

ALS	Approach and Landing System
API	Application Programming Interface
C/A	Coarse Acquisition
CAD	Computer-Aided Design
CALLISTO	Cooperative Action Leading to Launcher Innovation for Stage Tossback Operation
CNES	French National Center for Space Studies *French: Centre National d'Etudes Spatiales*
COTS	Commercial Off-the-Shelf
CPU	Central Processing Unit
CSG	Guiana Space Center *French: Centre Spatial Guyanais*
DAU	Data Acquisition Unit
DC	Direct Current
DC/DC	DC-to-DC
DGNSS	Differential GNSS
DGS	DGNSS Subsystem
DLR	German Aerospace Center *German: Deutsches Zentrum für Luft- und Raumfahrt e. V.*
DoF	Degrees of Freedom
DOP	Dilution of Precision
DR	Downrange
ECEF	Earth-Centered Earth-Fixed
EMI	Electromagnetic Interference

Revised paper as of October 21, 2019
[1] rene.schwarz@dlr.de, ORCID: 0000-0002-8255-9451
[2] marco.solari@dlr.de
[3] bronislovas.razgus@dlr.de
[4] matias.koerner@dlr.de
[5] benjamin.braun@dlr.de, ORCID: 0000-0002-0193-6607
[6] michael.dumke@dlr.de, ORCID: 0000-0002-5587-7884
[7] markus.markgraf@dlr.de
[8] martin.reigenborn@dlr.de
[9] jan.sommer@dlr.de, ORCID: 0000-0003-2815-0337
[10] dennis.pfau@dlr.de
[11] thomas.thiele@dlr.de
[12] johannes.riehmer@dlr.de

Eu:CROPIS	Euglena and Combined Regenerative Organic Food Production in Space
EVEREST	Evolved European Reusable Space Transport
FADS	Flush Airdata Sensing
FCS/A	Flight Control System/Aerosurfaces
FCS/R	Flight Control System/Reaction Control System
FCS/V	Flight Control System/Thrust Vectoring
FDIR	Failure Detection, Isolation, and Recovery
FDR	Flight Data Recorder
FEE	Front-End Electronics
FoV	Field of View
FPGA	Field-Programmable Gate Array
G&C	Guidance and Control
GNC	Guidance, Navigation and Control
GNSS	Global Navigation Satellite System
GPIO	General-Purpose Input/Output
GPS	Global Positioning System
GSOC	German Space Operations Center
HiL	Hardware-in-the-Loop
HNS	Hybrid Navigation System
IEEE	Institute of Electrical and Electronics Engineers
IMU	Inertial Measurement Unit
iNET	Integrated Network Enhanced Telemetry
iNET-X	iNET Extended
JAXA	Japan Aerospace Exploration Agency *Japanese:* 宇宙航空研究開発機構
LEO	Low-Earth Orbit
LFBB	Liquid Fly-Back Booster
LH2	Liquid Hydrogen
LNA	Low-Noise Amplifier
LOx	Liquid Oxygen
MECO	Main Engine Cut-Off
MVM	Mission Vehicle Management
OBC	On-Board Computer
OBCDH	On-Board Computing and Data Handling
OR	O-Ring
OUTPOST	Open modUlar sofTware PlatfOrm for SpacecrafT
PDR	Preliminary Design Review
PDU	Power Distribution Unit
PDU-C	PDU Controller
PDU-M	PDU Monitor
PPS	Pulse Per Second
PR	Pseudorange
PRR	Pseudorange Rate
PTP	Precision Time Protocol
PVT	Position, Velocity, and Time
RAAF	Royal Australian Air Force
ReFEx	Reusability Flight Experiment
RLV	Reusable Launch Vehicle
RTCM	Radio Technical Commission for Maritime Services
RTEMS	Real-Time Operating System for Multiprocessor Systems
RTK	Real-Time Kinematic
RTLS	Return-to-Launch-Site
SHEFEX II	SHarp Edge Flight EXperiment II
SMP	Symmetric Multiprocessing
SPP	Single Point Positioning
TC	Telecommand
TM	Telemetry
TM/TC	Telemetry and Telecommand
ToF	Time of Flight
UAS	Unmanned Aerial System
UAV	Unmanned Aerial Vehicle
UDP	User Datagram Protocol
VEB	Vehicle Equipment Bay
VTHL	Vertical Takeoff, Horizontal Landing
VTVL	Vertical Takeoff, Vertical Landing
WGS84	World Geodetic System 1984

1. Introduction

In order to bring reusable space transportation systems back to Earth, determining and actively controlling the flight state (that is, position and attitude) is essential. These capabilities are usually provided by Guidance, Navigation and Control (GNC) systems implemented aboard the spacecraft. One of the functions required and provided by GNC systems is the *navigation function*, which is responsible for estimating position, velocity, attitude, angular velocity, and other parameters of the flight state. Especially the final flight phase of reusable space transportation systems with approach to and landing in/on a predefined area or platform demands a challenging navigation accuracy, which cannot be achieved by conventional navigation systems.

Traditionally, the navigation of space transportation systems is realized by sole use of inertial measurements and is, thus, subject to drift due to continuous numerical integration of small measurement errors of acceleration and angular velocity into progressively increasing estimation errors of velocity, position, and attitude. This way, the accuracy of the navigation solution rapidly deteriorates over time and mainly depends on the quality of the Inertial Measurement Unit (IMU). The advantage of those systems is that they do not rely on any external reference, which makes them immune to interferences, jamming, or spoofing. The drawback is that — even with highest grade IMUs — the achievable navigation performance reaches a very low accuracy within a few minutes after system initialization, which is still enough for placing payloads into the desired orbit with sufficient accuracy, but inacceptable when space transportation systems shall be returned back to Earth with pinpoint landing capability.

Reusable Launch Vehicles (RLV), thus, require more advanced navigation approaches such as hybrid navigation. The term *hybrid navigation* refers to the combination of high-frequency inertial measurements with (generally lower frequency) data of other sensors like Global Navigation Satellite System (GNSS) receivers, radar and

laser altimeters, Sun sensors, star trackers, etc. by means of data fusion. Those sensors provide absolute measurements of certain physical quantities (e. g., position, velocity, orientation with reference to other objects, etc.) and enable to periodically correct for estimation errors resulting from the previously described integration drift mechanism. This way, the calculated navigation solution can be kept long-term stable. This approach also allows for lowering IMU performance requirements while still achieving a superior medium- and long-term navigation accuracy compared to purely inertial navigation systems.

The Department of GNC Systems of the DLR Institute of Space Systems develops such novel, autonomous Hybrid Navigation Systems (HNS). The development of the HNS technology for space transportation systems started already back in 2007 at DLR [1–4] and has been successfully demonstrated in the frame of the SHarp Edge Flight EXperiment II (SHEFEX II) mission and its flight in June 2012 [5–8]. HNSs are currently being developed as operational navigation systems in the frame of two RLV missions with different landing approaches: ReFEx (Reusability Flight Experiment), which is a DLR technology demonstrator for the development of key technologies for winged Vertical Takeoff, Horizontal Landing (VTHL) RLV, and CALLISTO (Cooperative Action Leading to Launcher Innovation for Stage Tossback Operation), a joint project of the French National Center for Space Studies (CNES), DLR, and the Japan Aerospace Exploration Agency (JAXA) for the development of a Vertical Takeoff, Vertical Landing (VTVL) RLV. The core technology is shared across these developments, but the specifically chosen sensor suite deviates significantly between the two HNSs due to major differences of the mission requirements.

The HNS development is supported by major contributions from the GNSS Technology and Navigation Group of the German Space Operations Center (GSOC) at DLR's Facility for Space Operations and Astronaut Training with the design and development of the GNSS subsystem and from the On-Board Software Systems Group of the Department of Software for Space Systems and Interactive Visualization at DLR's Facility for Simulation and Software Technology with the design and development of the base software running on the On-Board Computers (OBC) of the HNS.

This paper takes the developments in both of these missions as an example and describes the challenges faced for the development of navigation systems for VTHL and VTVL RLV. It provides an overview of the principal HNS architecture, which is commonly developed for both missions, and presents the selected sensor suites with GNSS, Differential GNSS (DGNSS), Sun sensors, laser and radar altimeters, and Flush Airdata Sensing (FADS) systems as non-inertial sensors including the required ground-based means and infrastructure. The paper concludes with a preliminary assessment of the achievable navigation performance for each of these missions.

2. Recent HNS Applications for RLV Missions

2.1. CALLISTO

In order to make access to space more affordable for both scientific and commercial activities, CNES, DLR, and JAXA joined in a trilateral agreement to develop and demonstrate the technologies that will be needed for future reusable launch vehicles. In the joint project Cooperative Action Leading to Launcher Innovation for Stage Tossback Operation (CALLISTO), a demonstrator for a reusable VTVL rocket, acting as first stage, is developed and built. As long-term objective, this project aims at paving the way to develop a rocket that can be reused. The combined efforts of the three agencies will culminate in a demonstrator that will perform its first flights from the Guiana Space Center (CSG) in Kourou, French Guiana.

The main objective pursued by CALLISTO is the collection of technical and economical data with reference to the development and operation of a reusable launcher first stage. For this purpose, the capability of flying, recovering, and reusing a vehicle under representative conditions of an operational system shall be demonstrated. This implies achieving to master the key technologies needed for future VTVL RLV, such as approach

Figure 1: Computer-Aided Design (CAD) rendering of CALLISTO.

and landing systems, retro-propulsion, cryogenic propellant management during highly dynamic maneuvers, and GNC, among others, in a relevant environment. CALLISTO is designed to mimic a vehicle architecture similar to an operational launcher which is capable to fly several times. The components used must thus either be completely reusable or easily refurbishable.

The CALLISTO vehicle is 13.5 m high, has a diameter of 1.1 m, and its mass at lift-off is less than 4 t. The vehicle is composed of five primary sections (from the top to the bottom; cf. Figure 3): The *Fairing* provides an aerodynamic cover for the upper vehicle body, especially for the ascent phase. It houses a GNSS antenna integrated into the nose tip. The fairing is connected to the *Vehicle Equipment Bay (VEB)*, which accommodates the Flight Control System/Aerosurfaces (FCS/A), major parts of the vehicle avionics, including, among others, the OBC, the HNS, Flight Data Recorder (FDR), Data Acquisition Units (DAU), as well as the Flight Control System/Reaction Control System (FCS/R) including its tank in the upper part. The fairing and the VEB form the so-called Top Module. The Top Module is followed by the *Liquid Oxygen (LOx)* and *Liquid Hydrogen (LH2)* tank sections, which provide the propellants for the engine. In the lower part of the vehicle, an *Aft Bay* houses the rocket engine itself, the Flight Control System/Thrust Vectoring (FCS/V), additional avionics, and interfaces for the Approach and Landing System (ALS). The Aft Bay and the ALS form the Bottom Module.

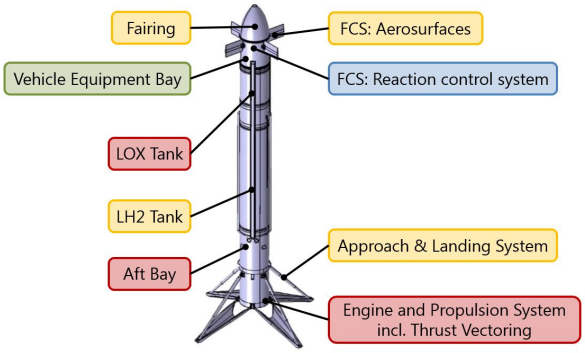

Figure 3: CALLISTO Vehicle Layout

The HNS is distributed to three of these sections: The HNS Box, the central part of the HNS, is accommodated within the VEB, while the GNSS antenna is integrated into the fairing and the radar altimeters are located outside on the Aft Bay.

The reusability of CALLISTO allows for an affordable incremental test approach with increasing flight envelope and complexity. It is foreseen to conduct at least ten flights with CALLISTO, beginning with very low energy hop flights up to full demo flight profiles with conditions expected to be representative and particularly critical for a reusable first stage (cf. Figure 2). All flights will be launched from CSG. The test flights will return back to landing pads on mainland, while the vehicle will land on

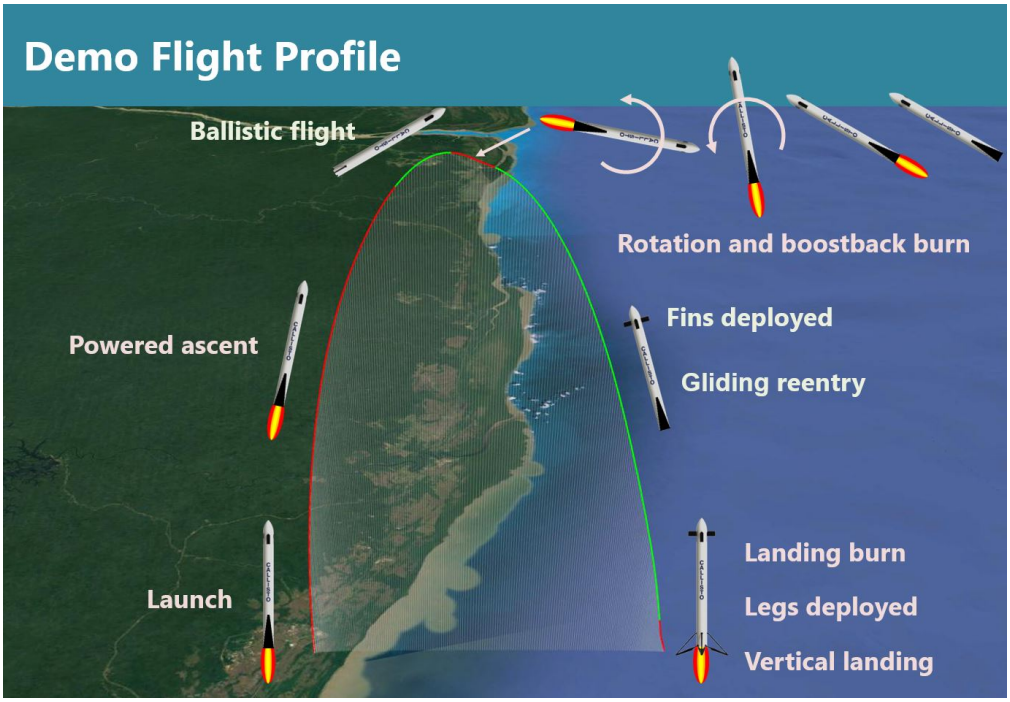

Figure 2: CALLISTO demo flight trajectory. Source: [9, supplemental conference material]

a fixed platform in the open sea off the coast of French Guiana during the demo flights. An alternative landing option for the demo flights is a floating barge instead of a fixed platform; the trade-offs concerning this matter are not yet concluded.

The project is currently in Phase B with the System Preliminary Design Review (PDR) scheduled later this year. More details on the mission, its background and objectives, on other key technologies as well as on further related aspects can be found in [9, 10].

2.2. ReFEx

DLR is developing the Reusability Flight Experiment (ReFEx), which is a sub-scale demonstrator representing a winged first stage of an RLV. It has a mass of around 400 kg and is approximately 2.7 m in length with wings spanning about 1.1 m (cf. Figure 4). The mission shall enable the development of key technologies necessary for future RLV applications, culminating in their demonstration with a controlled autonomous return flight in a representative scenario.

The main goal of the project is the demonstration of an autonomous re-entry flight of a winged vehicle from hypersonic velocity down to subsonic range. One of the main challenges is the vehicle design that enables a static as well as a dynamic stability of the vehicle in all these flight regimes. This imposes demanding requirements to the vehicle's aerodynamic design as well as the GNC subsystems. Especially the transonic region is challenging, since the position of the aerodynamic center of pressure will rapidly change. The development and demonstration of the corresponding GNC technologies is therefore a central part of the project.

ReFEx shall be launched by a Brazilian solid propellant two-stage VSB-30 rocket from the Royal Australian Air Force (RAAF) Woomera Range Complex, Australia.

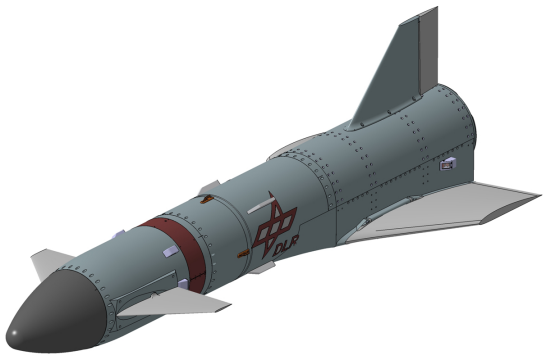

Figure 4: Configuration of the ReFEx payload during re-entry.

Following a guided rail travel, the launch vehicle builds up a roll rate aiming to reduce dispersion at payload separation and stage impact. First, the vehicle is unguided and passively stabilized by sets of four fins on each stage. To fulfill the flight stability requirement without major modifications on the launch vehicle, the effective aerodynamic surfaces of the ReFEx payload have to be reduced, which is realized by a foldable wing design and a 0.64 m diameter hammerhead fairing covering the tail section of the ReFEx experiment during atmospheric ascent. In the exoatmospheric flight phase after burn-out of the second stage, a yo-yo system is activated for despin and subsequently the stage is separated from the ReFEx payload.

After separation, ReFEx shall perform a re-entry similar to that of full-scale winged reusable stages. An RLV re-entry corridor was derived based on former research on the Liquid Fly-Back Booster (LFBB) [11] and other winged RLV concepts (e. g., Evolved European Reusable Space Transport (EVEREST) [12]). The mission goal of ReFEx is to achieve a re-entry trajectory in or close to this RLV corridor.

Thus, after despin, the vehicle is prepared for the atmospheric entry phase in which the vehicle is controlled by aerodynamic control surfaces (canards and rudder). In the first phase, ReFEx will fly in "belly-up" configuration with the fin pointing down. At a velocity of approx. 2 Ma, a 180 deg roll is performed and the atmospheric flight is continued with the fin pointing up. Finally, ReFEx will pass the transsonic regime and will continue on a glide path down to the ground. A sequence of the mission events is shown in Figure 5. More detailed information about the mission can be found in [13].

3. Core Building Blocks of the Hybrid Navigation System (HNS)

The HNSs developed by DLR are standalone systems meant for integration into distributed GNC systems. They typically implement the following fundamental functions:

1. *Navigation as Part of the GNC Chain*
   Providing an estimation of the vehicle state as feedback to the other elements of the GNC chain, and therefore closing the GNC loop, is the main purpose of the HNS. It does so by providing a high-frequency navigation solution to the vehicle computer. The HNS includes all necessary sensors and support electronics within its system boundaries.

2. *Time Reference/Synchronization*
   The HNS establishes the time reference for the entire vehicle and provides two means for time synchronization: For absolute synchronization of

time, the navigation message contains a date and time field. A dedicated electrical square wave signal accurately repeating once a second, called a Pulse Per Second (PPS), is generated by the HNS and can be used for phase and frequency synchronization between all clocks aboard the vehicle. If the HNS is connected to the avionics via Ethernet, the time can also be distributed via the standardized Precision Time Protocol (PTP) as defined by IEEE 1588-2002, whereas the HNS will serve as the PTP master within the avionics network, to which all connected avionics units can synchronize.

3. *Navigation for Flight Safety Purposes*
To provide another source of information about the vehicle state for flight safety purposes, the HNS sends the estimated vehicle's position and velocity via a Telemetry and Telecommand (TM/TC) gateway to ground. These messages are provided at a lower rate than the navigation solution for Guidance and Control (G&C) purposes and contain both the fused estimates based on all available sensors and the unprocessed information from the Position, Velocity, and Time (PVT) solution of the GNSS receivers. This is because the HNS itself is a technology demonstration, while the GNSS receiver technology is flight proven in many DLR missions and, thus, considered as very reliable. The receiver output is independent of the remaining HNS, despite of the powering via the internal Power Distribution Unit (PDU).

4. *Navigation for Correlation of Experimental Data*
The navigation solution is used to correlate experimental data with navigation information. It is probably provided in a lower frequency than the navigation solution used for G&C.

The heart of the HNS is a central electronics unit (called "HNS Box"), which houses a tetra-axial IMU consisting of four accelerometers and four gyroscopes, the navigation on-board computing and data handling components, the internal PDU, the GNSS receivers, and auxiliary electronics. It is designed internally in form of a hot-redundant fail-operational system architecture with Failure Detection, Isolation, and Recovery (FDIR) mechanisms both in terms of hardware and software to increase reliability and robustness against most outages or failures of individual sensors and components. External sensors are connected via serial communication links directly to the HNS Box, which supplies them with the required power at the same time. The HNS Box has there-

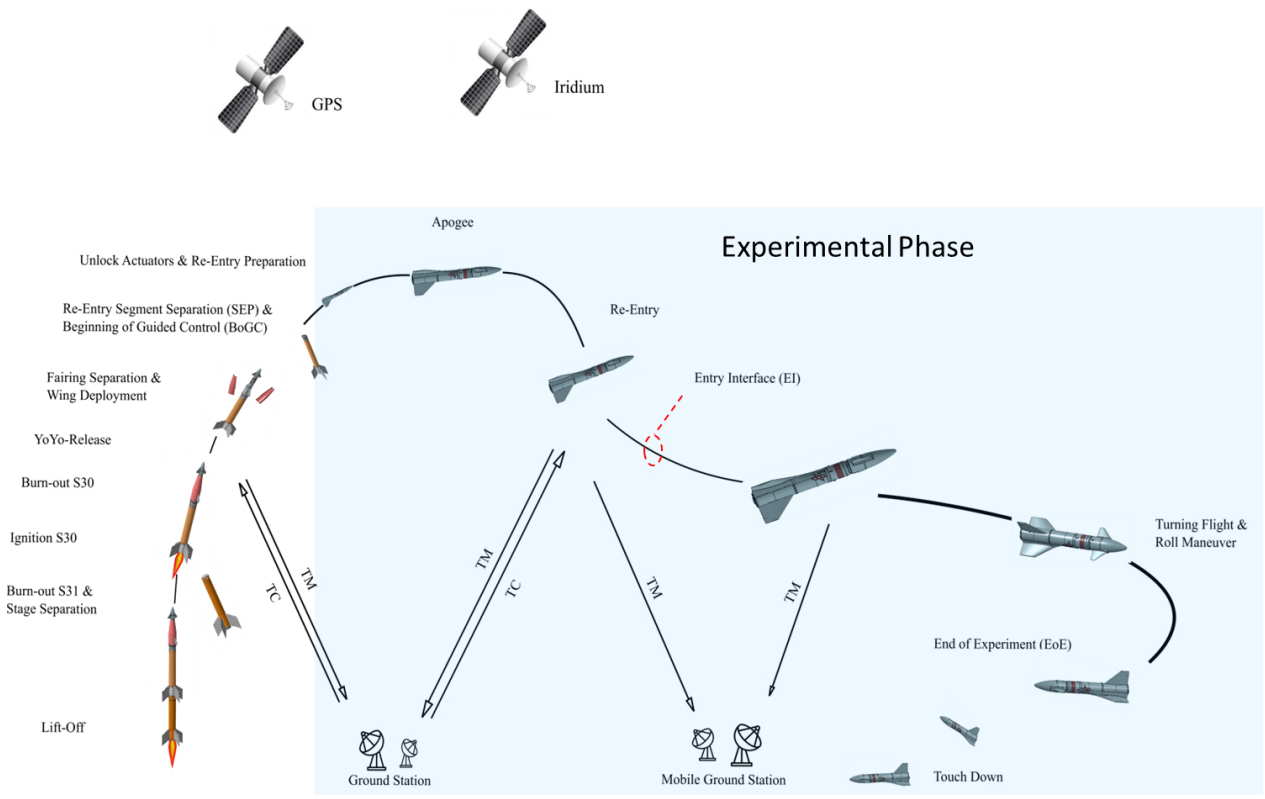

Figure 5: Overview of the ReFEx mission sequence.

fore also the possibility to closely monitor the behavior of the external components and can power cycle or permanently turn them off in case of anomalies.

The HNS Box is integrated in the vehicle interior and connects to the other vehicle avionics via an Ethernet or serial (RS-422) communication link. Aside from the IMU and GNSS receivers as core sensors integrated into the HNS Box, the HNS is capable of being equipped with additional external sensors (like Sun sensors, laser and radar altimeters, star trackers, etc.), depending on the mission needs. These sensors are usually connected via serial RS-422 links to the HNS.

Thanks to the modularized system and software design as well as the powerful OBCs, functionalities extending beyond the aforementioned fundamental functions (see Section 4.1 for examples) can be implemented according to the mission needs.

3.1. Inertial Measurement Unit

The proper functioning of the IMU is vital for the navigation system as the high-rate measurements of angular velocities and linear accelerations, integrated to generate a position, velocity, and attitude solution, ensure the continuity of the navigation output. This continuity is fundamental since possible gaps in the measuring of the high dynamics experienced by RLVs could cause large losses in navigation solution accuracy which in turn could lead to unrecoverable flight states. The IMU is designed as tetra-axial configuration of four Commercial Off-the-Shelf (COTS) gyroscopes and four COTS analog accelerometers with an in-house developed Front-End Electronics (FEE). This design allows a partly redundant linear acceleration and angular velocity measurement scheme, thus offering an over-determined measurement system for the three spatial axes. In the event of failure of one sensor, the remaining three sensors will still cover all three spatial axis. All components are mounted onto a self-developed mechanical structure.

3.2. On-Board Computing & Data Handling

In order to enable the HNS to perform all its functions, a highly reliable, fault-tolerant On-Board Computing and Data Handling (OBCDH) architecture with the necessary infrastructure components (e. g., a fully redundant PDU) incorporating a FDIR scheme is being developed. Its key characteristic is an augmented, double modular hot-redundancy scheme of two OBC nodes. The OBCs are stackable COTS single-board computers with Intel Atom Quad-Core Central Processing Units (CPU) in the standardized PC/104-Express format. The OBC stacks are extended with custom interface extension boards based on a Xilinx Spartan-6 Field-Programmable Gate Array (FPGA), providing a large amount of RS-422/485 serial communication links, General-Purpose Input/Outputs (GPIO), and Ethernet ports. Each OBC stack will be supplied by one in-house developed power supply board.

The OBCs are operated in a hot redundancy scheme, i. e., each OBC receives the data of all components and performs all calculations with the same on-board software. However, only one OBC is the *currently active OBC* whose outputs (commands) will be routed to the respective components within the HNS or to the outside world (i. e., the navigation solution, telemetry, etc.). All outputs of the other OBC (referred to as *standby OBC*) are suppressed by an electronic circuitry. In case of failure of the currently active OBC, the system can switch the roles of both OBCs, so that the output of the previous standby OBC will be routed. After switching the roles, the failing OBC will be power cycled and tested. There are various failure detection mechanisms in place in order to ensure a proper and timely role switch in case of failures.

The OBCDH systems closely interact with the PDU, which is controlled by the OBCs and delivers valuable monitoring data back. This way, it is also possible for the OBC to detect power anomalies and switch certain devices on or off to safeguard or recover the system operation. The PDU also plays a vital role for initialization of the HNS as it ensures a sequential and proper activation of all components, especially the OBCs.

3.3. Power Distribution

The PDU is the internal power supply for the HNS and is located within the HNS Box. It monitors and controls the supplied power for all devices belonging to the HNS. Since it is a 1-fault-tolerant power supply, a redundancy concept for its critical parts has been implemented [14–16]. The PDU Monitor (PDU-M) monitors currents, voltages, and temperatures within the HNS and transmits this information to the PDU Controller (PDU-C) to control each power channel output [17]. As an additional feature, all power channel outputs have an overvoltage protection.

The PDU has, among others, Electromagnetic Interference (EMI) filters, resettable electronic fuses, electronic switches, DC-to-DC (DC/DC) converters and O-Ring (OR) diodes. EMI filters prevent the DC/DC converters' high-frequency currents to flow back to the vehicle power supply. Electronic resettable fuses protect each power switch against overcurrent. In case of an overcurrent condition, the fuses can be resetted by switching off and on the corresponding electronic switch. Primary switches control the DC/DC converters and secondary switches control the HNS devices supplied power, re-

spectively. The DC/DC converters reduce the power bus voltage level coming from the vehicle power supply to the required ones. OR diodes isolate the DC/DC converter outputs to achieve a redundant output connection [18]. Figure 6 shows the basic PDU block diagram.

The redundant PDU concept enables the HNS devices to receive power from their redundant supply lines during an electronic switch failure. In addition, the PDU detects errors in the PDU-C through its watchdog circuitry when no or wrong stimuli signals are produced. The fail-safe mode procedure takes place when the PDU-C fails and activates all power channels outputs in consequence. Therefore, all HNS devices are powered. If the fail-safe mode is initiated, the electronic switches cannot be controlled anymore. However, since at this stage all HNS devices are switched on, the overall system operation is not affected [4].

The PDU design is slightly adapted for each mission in order to provide the required amount of power channels and electronic power switches corresponding to the equipped components.

3.4. Base Software

The on-board software of the HNS OBCs needs to fulfill a number of complex tasks in a guaranteed time. This includes beside the navigation functionality itself, the distribution of the on-board time to other subsystems, and the generation of telemetry data, both live data for immediate downlink as well as high-rate data for post-flight analysis. The Base Software includes most notably the operating system including mission-specific drivers, the hardware abstraction, the execution runtime for the navigation algorithms and the background services for communication with other subsystems, e. g., the distribution of the global time reference.

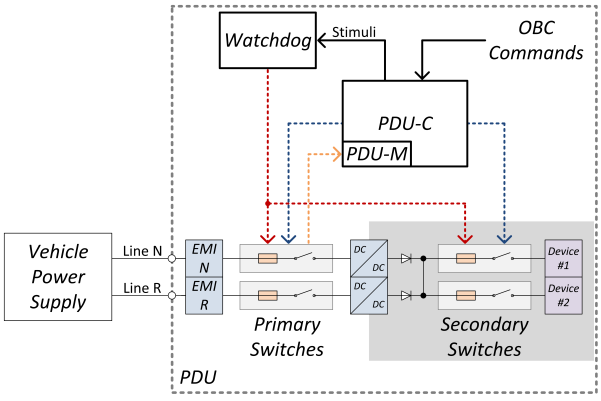

Figure 6: PDU Block Diagram

3.4.1. Operating System

All of the above mentioned services need eventually be supported by the underlying Base Software and in turn drive its design decisions. Firstly, the state estimation of the HNS including the triggering of sensors and processing of measurement data need to be executed in precise time windows. Therefore, the Base Software support for execution in a real-time context is a key requirement. The algorithms are expected to be complex with regard to the computational performance requirements. That means, the Base Software needs to provide enough computational reserves by fully supporting the multicore CPUs of all OBCs and the distribution of software tasks among those cores. Naturally, the Base Software needs to implement drivers for all low-level interfaces which are used for communication with connected sensors and actuators or other remote terminals.

Based on those basic requirements, Real-Time Operating System for Multiprocessor Systems (RTEMS) [19] was selected as operating system. It is an open source real-time operating system which supports a large set of different hardware architectures and with a long heritage in space-related applications. In its most recent version, it provides a real-time executive and real-time schedulers for Symmetric Multiprocessing (SMP) on multicore systems. The programming interface even supports multiple scheduling groups and thread pinning for distributing the workload among the processor cores with certain constraints [20]. However, the RTEMS port for x86-based hardware platforms did not have a functional implementation of the SMP scheduling system. Therefore, as a first development step, the code base has been extended to support SMP for the x86-based OBCs of the HNS. The open source nature of RTEMS also allows to integrate drivers for the custom-made interface board of the HNS OBC which are the basis for the communication with sensors and other subsystems.

3.4.2. Middleware

The planned development cycle for the on-board software is comparably short and available development resources are limited. With all OBCs being based on the x86 architecture, the goal is to share as much code as possible among them and reuse existing DLR software technologies where suitable. That means, the OBCs of the HNSs will use the same operating system but with differing mission-specific driver implementations as their interface devices are not completely the same. The middleware layer is responsible for hardware abstraction and providing an execution runtime for the application layer software. The hardware abstraction is done in two steps. First, a common Application Programming Interface (API) for the actual interface devices is used in order

to separate the device time, e. g., serial connection from the low-level operating system driver. The second layer then uses this common API to provide access to connected devices to the application layer. For the hardware abstraction layer, DLR's Open modUlar sofTware PlatfOrm for SpacecrafT (OUTPOST) library [21] will be used and extended with new interface and device drivers as needed.

The execution runtime for the navigation algorithms will be provided by DLR's own Tasking Framework [22] which has been successfully used in attitude control systems in previous missions, e. g., the Compact Satellite mission "Euglena and Combined Regenerative Organic Food Production in Space (Eu:CROPIS)" [23]. The algorithms themselves are partitioned into smaller stateless tasks which exchange data via one or multiple channels. The channels hold the input data or control the timed activation of the tasks' inputs. When all necessary inputs for a task are activated through available data or a timed event, a task is scheduled as soon as possible.

3.4.3. Development Methodology

The overall software development is carried out by a distributed team of developers and engineers, where most of them do not have direct access to actual flight hardware or a Hardware-in-the-Loop (HiL) setup for most of the time. Most parts of the middleware, i. e., the OUTPOST library and the Tasking Framework are implemented using a subset of the C++ programming language which encourages strong typing and most notably does not allow the use of dynamic memory allocation during runtime or the use of exceptions. Both libraries also use abstract classes for interface definition extensively, thereby enabling easy setup of test cases with mock classes for hardware devices in order to test higher level functions without flight hardware. They can both be compiled for the RTEMS real-time operating system and for common Linux workstations. This allows to write and execute large parts of the testsuite on common development workstations with a large set of development and analysis tools available and in turn reduce the amount of on-hardware testing significantly during the development phase.

4. Mission-Specific Adaptations and Extensions

Due to the differences in mission design and goals of both projects, the aforementioned core HNS building blocks are adapted and extended to satisfy the particular needs of the missions. The key drivers as well as the modifications and extensions theirselves are briefly described in the following subsections. Table 1 provides an overview of the differences between the two HNSs developed for CALLISTO and ReFEx.

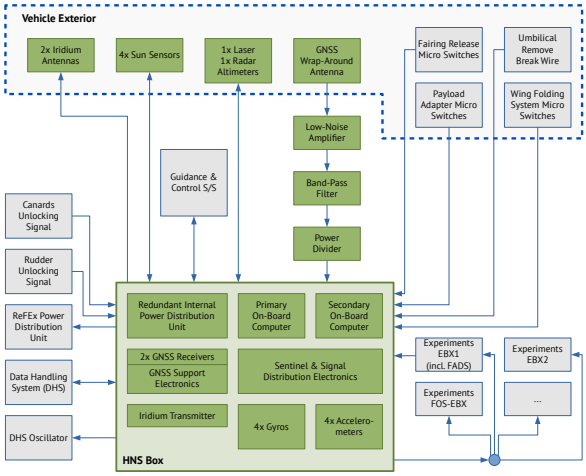

Figure 7: Overview of functional groups and components of the ReFEx HNS. The connections between the components represent the data flow without further distinction between signal types.

4.1. ReFEx

The ReFEx vehicle will be launched using an unguided two-stage VSB-30 rocket which is spinning up to approx. 4 Hz during the ascent phase to reduce the dispersion at the payload separation corridor. This high rotation rate causes the buildup of a signifcant attitude estimation error, which needs to be corrected. Sun sensors have been identified as suitable for this purpose.

Additionally, this high rotation rate would exceed maximum measurement rate of the gyros within the IMU. It turned out that the measurement range of the gyros could be extended by the manufacturer with smaller modifications to the standard commercially available version.

A flare maneuver shall be carried out shortly before landing of ReFEx to reduce the remaining energy of the impact. For this maneuver, an estimation of the flight altitude above ground is required. Since ReFEx is not designed to land softly, the requirement for flight altitude estimation accuracy is not as high as compared to CALLISTO. A combination of a laser altimeter and a radar altimeter resulted as the most suitable solution. The refresh rates of the sensors are high enough to allow maneuvering into a flare maneuver with high vertical speeds. Both solutions can operate free of ground infrastructure and can be easily integrated into the vehicle. The integration of the sensors into the vehicle is flexible due to the variety of available COTS products with sufficient measurement accuracies. A vacuum and thermal protection will be implemented for the sensors.

To support the vehicle recovery, the HNS shall transmit the vehicle position via an independent communication channel to ground. An Iridium transceiver has been included in the HNS to cover this functionality.

Since Telemetry (TM) bandwidth is limited, only the most relevant data can be transmitted during flight. To enable an extended post-flight analysis, high-rate measurement data is saved to an impact-resilient data storage within the HNS Box, which is recovered after landing.

In order to coordinate the operational state of all subsystems, a Mission Vehicle Management (MVM) is implemented within the HNS. This MVM collects and evaluates information from sensors and — while on ground — manual commands from operators to switch between predefined modes of operation. The information about the current mode of operation is distributed to all subsystems as part of the navigation solution to avoid additional interfaces.

Figure 7 provides an overview about the hardware archiecture of the ReFEx HNS.

4.1.1. GNSS Subsystem

The GNSS subsystem of the ReFEx HNS is based on the flight-proven Phoenix-HD Global Positioning System (GPS) receiver (Figure 8 (top)) developed at DLR/GSOC specifically for use in space and high-dynamics projects [24, 25]. The Phoenix-HD offers single-frequency Coarse Acquisition (C/A) code and carrier phase tracking on 12 channels and can be aided with either real-time, or alternatively, a priori trajectory information to safely (re-)acquire GPS signals even at high velocities and accelerations. The receiver is based on a check-card-sized commercial hardware platform [26], built around the GP4020 baseband processor of Zarlink, combined with a firmware developed by the GNSS Technology and Navigation Group at DLR's GSOC for space applications. The receiver was successfully employed in several dozens of national and international sounding rocket, launcher, and Low-Earth Orbit (LEO) satellite projects over the last decade. The receivers will provide position and velocity fixes as well as GPS raw data (pseudoranges and range rates) to the navigation computers for fusion with data from other position and attitude sensors. Moreover, the GNSS subsystem will provide timing information in terms of a PPS signal and corresponding time messages to the vehicle.

A redundant pair of Phoenix-HD receivers will be accommodated in a common enclosure along with an electrical interface board specifically designed and build for this mission. The design of this so-called GPS main electronic unit has been chosen such that in future projects utilizing the HNS modifications, e. g., of the employed navigation receivers or the redundancy concept, can be applied without the need to also change the electrical or mechanical interface of the main electronic unit.

For the reception of GPS signals during the flight, a single GNSS wrap-around antenna (Figure 8 (bottom))

	CALLISTO	**ReFEx**
Base Box Modifications	GNSS receivers replaced by COTS multi-constellation, DGNSS-enabled receivers	Measurement range extension of gyros in IMU to ±1,500 °/s; impact-resilient data storage and Iridium transceiver included
GNSS Subsystem	Differential multi-constellation multi-frequency design with reference stations at all landing sites	Flight-proven Phoenix-HD
GNSS Antenna	Hemispherical antenna integrated in nose cone	Wrap-around antenna around vehicle body
Radar Altimeters	High accuracy, customly developed	COTS UAV class sensors
Sun Sensors	—	Yes
Laser Altimeters	Experiment	Operational
FADS System	Yes	Yes
Interface to Avionics	UDP with iNET-X packetization standard on top of Ethernet	RS-422 serial

Table 1: Comparison of the HNS configurations for CALLISTO and ReFEx.

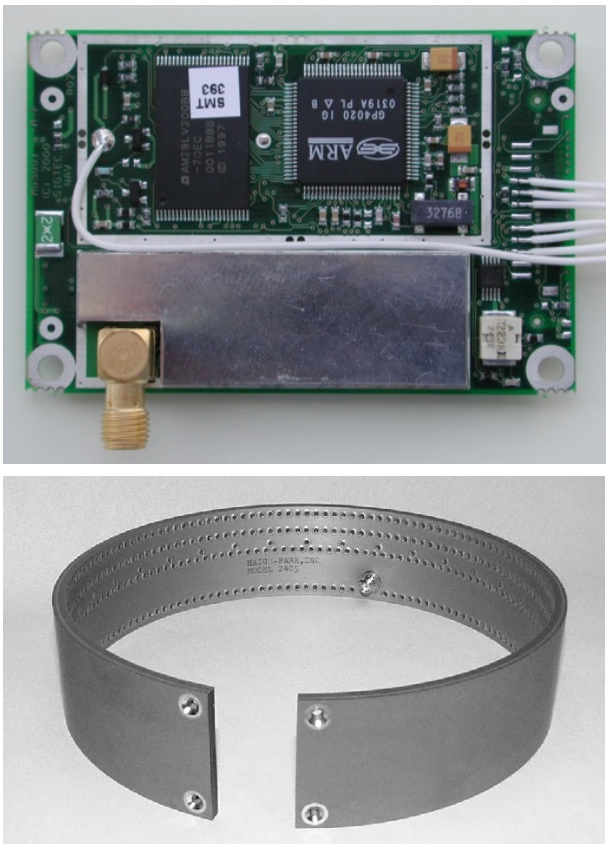

Figure 8: Core components of the GNSS subsystem of ReFEx: Phoenix-HD GPS receiver board (top) and example picture of a GNSS wrap-around antenna for sounding rockets and missiles (bottom).

will be used. The main advantages of this type of device are the almost omnidirectional receiving pattern as well as the spin-insensitivity of the antenna. It will be flush-mounted into the cylindrical part of the structure of the ReFEx re-entry vehicle in between the nose cone section and the wing section but outside of the fairing. The choice of a wrap-around antenna and the above mounting position allows for a proper signal reception, and thus availability of a valid GPS navigation solution, throughout all flight phases from lift-off to landing. In order the make the antenna resistant to the high temperatures expected during launch and re-entry, an ablative heat shield is added to the antenna by the manufacturer.

Figure 9 provides a structural overview of the complete GNSS subsystem architecture. In between the above already addressed wrap-around antenna and main electronic unit, a dedicated GPS Low-Noise Amplifier (LNA), also developed at DLR for space missions, and a COTS passive power divider will be inserted to complete the GNSS subsystem of the HNS for ReFEx. An optional match-box-sized GPS L1 band-pass filter may further be added in between the LNA and power divider in case GPS interferences are detected during the system-level tests to be conducted once all components and subsystems are available for such testing.

4.1.2. Sun Sensors

Digital two-axis COTS Sun sensors are utilized within the HNS sensor suite to aid the attitude estimation process, especially to reduce the estimation errors after the yo-yo despin maneuver. Four Sun sensors are equidistantly placed around the circumference of the longitudinal body axis of the vehicle. Each Sun sensor has a Field of View (FoV) of 120 deg in each axis and measures the Sun position with an accuracy better than 0.3° (3σ). The sensors are directly connected via dedicated RS-422 serial interfaces to the HNS Box, from which they are also powered.

4.1.3. Laser Altimeters

A laser altimeter will be part of the ReFEx sensor suite for the landing phase. The nature of the laser altimeter will output the distance between the emitting element and the ground in a straight line. Clearly, the attitude of the vehicle is taken into account to back-calculate the flight altitude over ground.

The laser altimeter will be mounted facing downwards during the landing phase, with a cutout in the main hull and a protective glass against the thermal loads during the re-entry phase. The selected laser altimeter has a range of 1,500 m and will operate as a single sensor down to an altitude of 100 m over ground, where the radar altimeter will start its operation.

4.1.4. Radar Altimeters

The ReFEx vehicle will also use a radar altimeter for the flare maneuver during the landing phase. While the laser altimeter is intended to be used during the early approach prior to landing, the radar altimeter will be used alongside during the final approach. The advantage of the radar altimeter comes from its operative nature, providing the altitude over ground as an output independently of the attitude over a flat area.

The radar altimeter is a COTS aeronautical sensor for UAV applications, offering heritage and reliability. The small package of the sensor eases the integration on to the outer shell of the vehicle, facing the ground during landing. Although, a thermal protection system will be implemented for the hypersonic and supersonic flight phases since the sensor casing is not designed for those flight regimes. The radar altimeter will operate during final the approach starting at an altitude of 100 m over ground with an update rate up to 800 Hz.

4.1.5. Flush Airdata Sensing (FADS) System

The Flush Airdata Sensing (FADS) system is used to determine the vehicle angle of attack, angle of sideslip, freestream static pressure and dynamic (impact) pressure using a matrix of six pressure orifices on the vehicle nose. The orifices are connected to the pressure sensors located in the nose section directly behind the nose tip via short metallic and flexible tubing. The short tubing length minimizes pneumatic lag and ensures a fast response time of the pressure measurement. The distribution of the pressure measurement locations on the spherical nose part depends on the maximum expected angle of attack and sideslip. The distribution is similar to the X-33 FADS system presented in [27] with one stagnation point measurement and five pressure ports distributed around the stagnation point on the vertical and lateral meridian.

The above-mentioned airdata parameters are calculated using the measured pressures and a dedicated software algorithm described in [27]. In addition to the pressure values, three calibration parameters are necessary for the algorithm which are determined by wind tunnel tests on a subscale model varying angle of attack, angle of sideslip, and Mach number in their respective ranges.

Pressure sensor data acquisition and algorithm execution are conducted by one of the two electronic boxes of the ReFEx flight instrumentation. The resulting values are provided to the HNS via serial communication line. Although the HNS also determines the airdata parameters, the values provided by the FADS system are used as a second source of information. In contrast to HNS, values calculated by the FADS system also include actual wind conditions at the vehicle location which is especially important at lower flight speed in the sub- and transonic regime.

4.2. CALLISTO

The challenging design drivers for the CALLISTO HNS development are mainly the requested accuracies for the estimation of the vehicle's altitude above the landing pad as well as of the horizontal position, especially during the last part of the flight for approach and landing. From the G&C studies conducted so far, a required estimation accuracy for the altitude of 0.5 m and for the horizontal position of 1.0 m has been derived. In terms of attitude, an estimation accuracy of 0.3° for the yaw and pitch axes and 0.5° for the roll axis is called, respectively, while the attitude rate estimation accuracy for all axes shall be better than or equal to 0.1 °/s. The velocity of the vehicle shall be estimated with at least 0.2 m/s accuracy. All aforementioned values are given at 99 % confidence and with the highest accuracy requested for each property from all flight phases.

A first assessment of the navigation performance showed that the HNS sensor suite already defined for ReFEx was not sufficient. Especially the requested accuracy for the estimation of the vertical and lateral position cannot be fulfilled out of the box. At first, the achievable performance improvements by enhanced GNSS solutions — in contrast to using a standalone single-constellation GNSS design used by ReFEx — has been

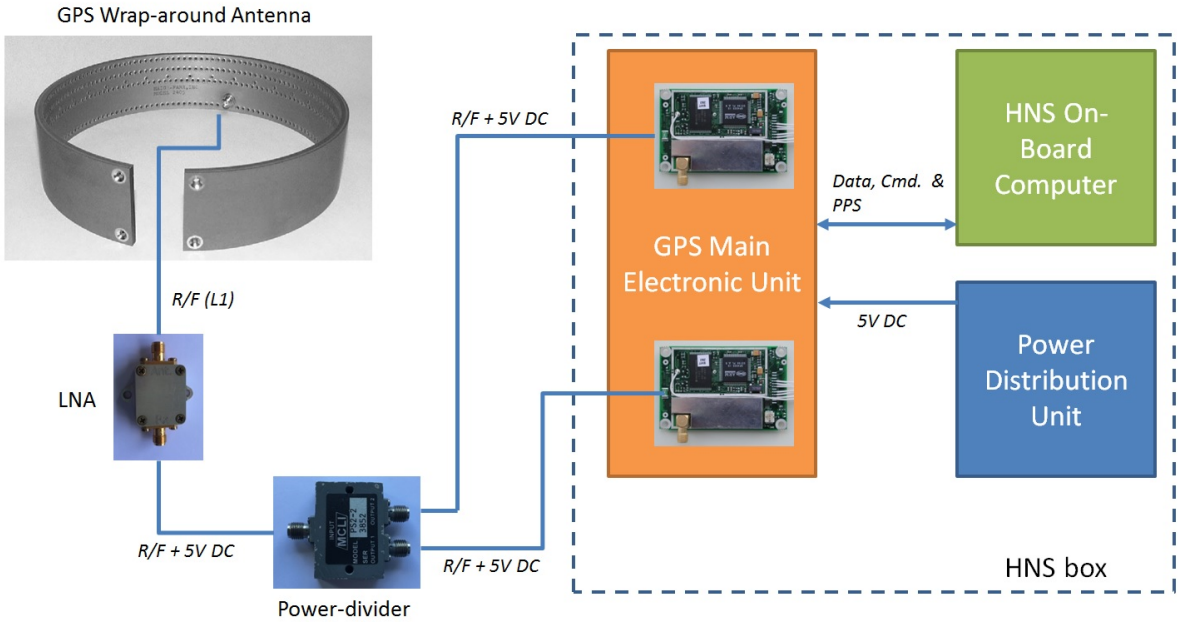

Figure 9: Structural diagram of the GNSS subsystem architecture for ReFEx.

studied. In the course of this study, the use of GNSS augmentation systems for flight altitude determination has been also considered, but the achievable accuracy, reliability, and robustness has been evaluated as unsuitable for the vertical navigation solution.

However, a suitable concept for improving the lateral channel was found with a DGNSS concept, which consists of GNSS receivers along with a suitable antenna aboard the rocket, reference GNSS receiver(s) and antenna(s) on ground near the landing site, and a telemetry uplink for real-time correction data. The GNSS antenna aboard CALLISTO requires a good FoV to the satellites during ascent, toss-back maneuver, and landing. Three antenna and accommodation options were considered: A single antenna integrated in the nose tip, two antennas mounted on the opposite sides of the rocket, or a wrap-around antenna. Out of these options, the nose tip antenna has been selected as baseline design.

The ground infrastructure for a DGNSS system increases the complexity of the CALLISTO system but it is seen as the sole solution to achieve the required navigation performance. On ground, DGNSS reference station(s) will provide corrections for Pseudorange (PR) and Pseudorange Rate (PRR) measurements for the DGNSS Subsystem (DGS) in Radio Technical Commission for Maritime Services (RTCM) format. If feasible and required, the reference station(s) can also generate data for Real-Time Kinematic (RTK) navigation. The reference station(s) are used for monitoring of jamming, spoofing, scintillation, and ionosphere.

For measurements of the flight altitude, evaluation was made on laser altimeters, radar altimeters, barometric altimeters, visual reference systems, GNSS receivers (including augmentation systems for satellite navigation), and beacon navigation. Finally, radar altimeters have been identified as the most feasible solution to enhance the vertical accuracy of the HNS. Radar altimeters are Time of Flight (ToF) sensors with electromagnetical carrier waves of frequencies in the range of $2-100$ GHz. They are common instruments within aeronautics used to measure the distance to the ground; they are also commonly used as highly reliable sensors for automatically landing aircraft. Typically, two antennas are necessary, separated for transmitting and receiving. The antennas can either be integrated within a common housing for antennas and electronics or separated from the electronics.

Furthermore, the radar altimeter is expected to be resistant against the plume/exhaust and dust interactions. Disadvantages like the accommodation on the vehicle, and the limited accuracy are probably much easier to overcome than to prove another technology ready for a rocket engine propelled vehicle like CALLISTO.

However, radar altimeters available as COTS devices for use by aircraft usually feature an accuracy within ± 1 to 3 ft $\pm$ 1 % of altitude (approximately ± 1.305 m for 100 m true altitude) in the best case. Such radar altimeters thus do not fulfill the accuracy requirements of CALLISTO and a custom radar development is currently being investigated. The selected baseline is the inclusion of two radar altimeters with integrated antennas to be accommodated on the outside of the Aft Bay.

4.2.1. Differential GNSS Subsystem

The CALLISTO DGS is an integral part of the HNS that provides a major source of navigation information for real-time guidance and control. Beyond that it provides relevant data for post-flight trajectory analysis and range safety. Within the HNS, GNSS provides the primary source for absolute position information but also contributes relative position information with respect to the landing side. GNSS tracking will cover all flight

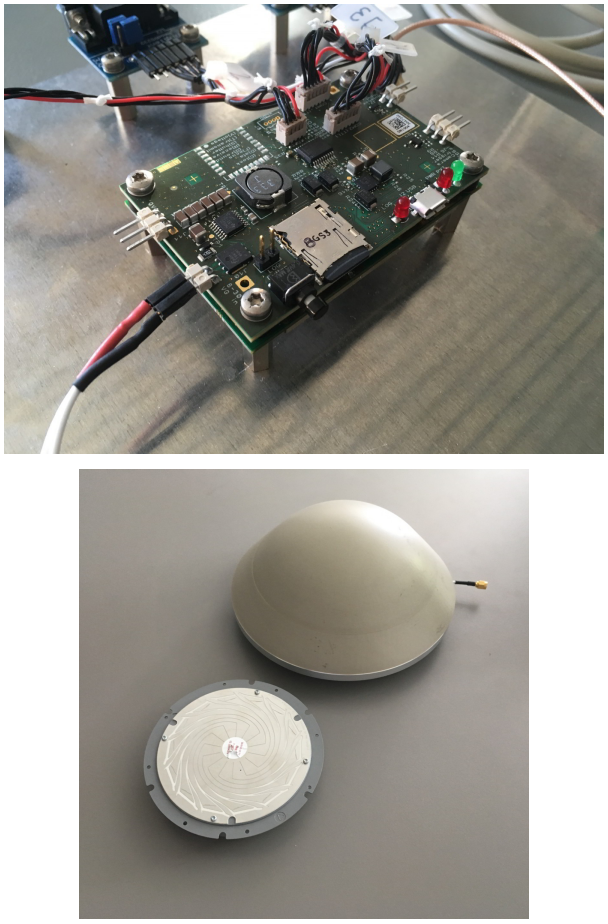

Figure 10: Core components of the DGNSS subsystem of CALLISTO: AsteRx-m2 multi-GNSS receiver including Unmanned Aerial System (UAS) extension board (top) and the nose cone antenna (bottom).

phases from launch to landing, which poses special requirements on the GNSS receiver in terms of tracking under high signal dynamics and the environmental conditions.

The DGS is based on a hot-redundant pair of GNSS receivers (Figure 10) offering dual-frequency GPS and Galileo tracking on two frequencies (L1/L2 and E1/E5a). In view of engineering budgets (mass, power, form factor, etc.), a tight project schedule, and cost considerations, COTS receivers will be used that offer a high maturity as well as adequate robustness. Based on flight heritage from the earlier use on an Ariane 5 vehicle [28], Septentrio AsteRx-m2 receivers have been selected as primary candidates for the CALLISTO mission and are presently undergoing further testing and qualification.

The GNSS receivers will be jointly connected to an active antenna via a power splitter. The antenna itself will be integrated in the nose cone of the CALLISTO vehicle to provide hemispherical coverage. It is based on a NovAtel pinwheel antenna element supporting survey-grade GNSS measurements across the L1/E1, L2, and L5/E5a frequency band. The pinwheel antenna design [29] allows operation of the antenna without a dedicated ground plane and offers a high level of multipath suppression. A prototype nose cone with the integrated antenna element and LNA as shown in Figure 10 is currently undergoing testing and calibration of gain and phase patterns to qualify the design for the CALLISTO mission.

Aside from the on-board components, the DGS also comprises at least one ground-based reference station near the landing site (Figure 11). This reference station will collect GPS and Galileo observations that will be sent to CALLISTO via a radio-frequency Telecommand (TC) uplink. This enables a differential correction of the on-board observations to achieve enhanced accuracy and meet the demanding horizontal positioning knowledge required during the landing phase. Depending on the specific choice of landing site (land, fixed platform, moving platform), a permanently installed GNSS monitoring station, a temporary but static reference station, or a small network of receivers for position and orientation determination of a moving barge can be foreseen.

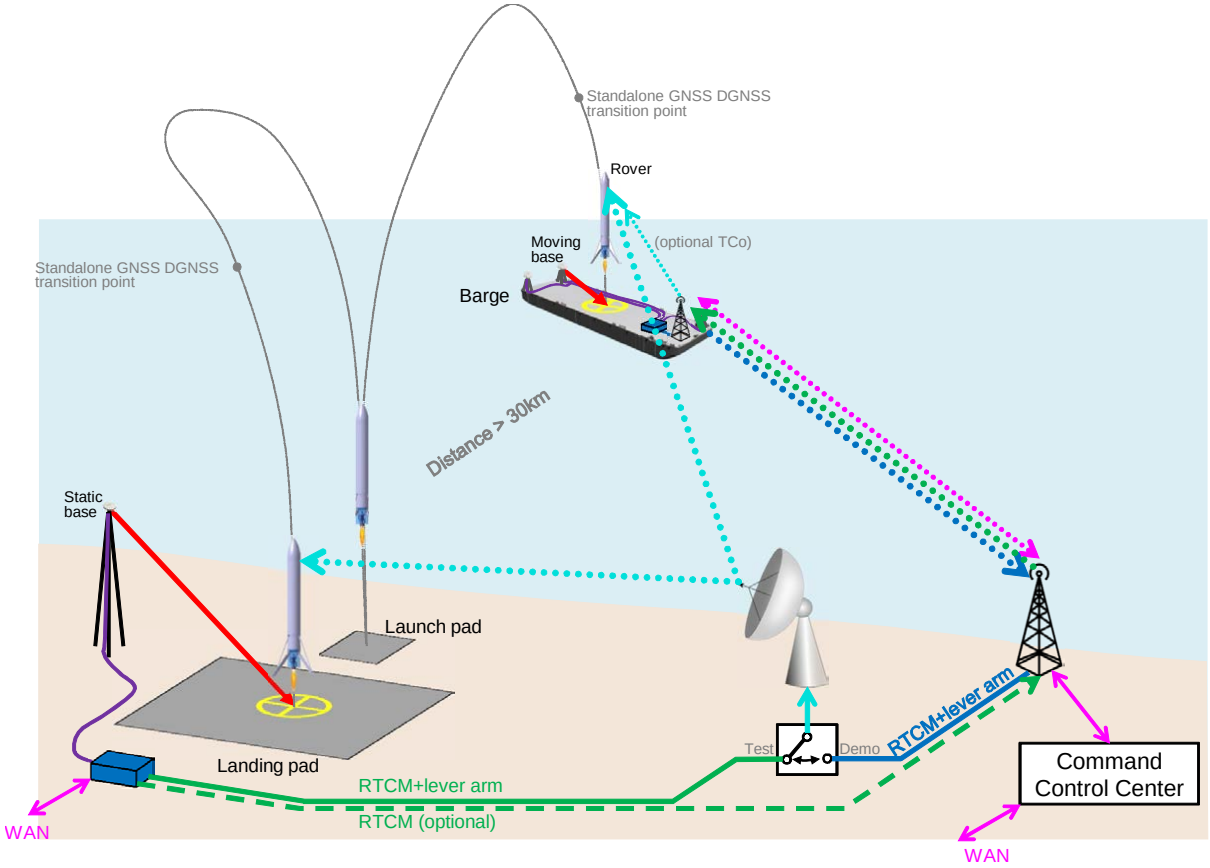

Figure 11: System architecture for absolute and DGNSS navigation during all flight phases of the CALLISTO vehicle.

4.2.2. Radar Altimeters

Previous analyses resulted in the selection of radar altimeters as the only satisfying solution for direct and high-accuracy measurements of the vehicle's flight altitude relative to the landing pad. As a side effect, radar altimeters are also capable of giving a direct measurement of the vehicle's approach velocity relative to the landing pad. However, there is no COTS radar altimeter solution available on the market which directly fulfills all requirements and constraints set by the mission. It is currently investigated whether and how existing radar sensors or technologies can be adapted for the CALLISTO HNS. Main challenges taken to be into account are

- the desired measurement principle,
- the unknown interaction of the signals with the engine plume, and
- the operational environment conditions arising from the accommodation.

Initially, a very simple measurement method similar to radar altimeters used for aircraft and UAVs was foreseen. In principle, such radar altimeters measure the distance between the aircraft and the terrain directly beneath it by sending out radio waves and measuring the time it takes to receive these signals back due to reflection on the ground (called Time of Flight (ToF)). Using the ToF measurement and the known speed of electromagnetic waves in air, the distance to ground can be calculated. In general, the ToF measurement is based on the first reflection received back, i. e., the nearest object within the spherical propagation direction whose radar cross section is large enough to be detected. This measurement principle would work for CALLISTO if the radar altimeter measurements would be needed only during a flight phase where the vehicle is already directly located above the landing pad, where the maximum tilt angle of the vehicle is smaller than the half beam angle of the antenna, and where no objects within the signal sphere tangent to the landing pad surface higher than the landing pad itself are present (cf. Figure 12 (left) for a visualization).

In the course of the further studies it turned out that the radar altimeter measurements are already needed at a point in time when the vehicle is not yet located directly above the landing pad, but with a horizontal distance of some hundred meters. In this situation, the altitude above the terrain beneath the vehicle instead of the altitude above the landing pad would be measured (cf. right side of Figure 12). Additionally, keeping the required area clear of any higher objects turned out to be challenging. It was then decided to discard this simple measurement principle in favor of a concept which relies on identification of the landing pad center in the radar signals.

In this more complex measurement scenario, radar reflectors are placed in the landing pad center and around it, which can be identified in the received radar signals by specialized detection algorithms. The antenna aperture

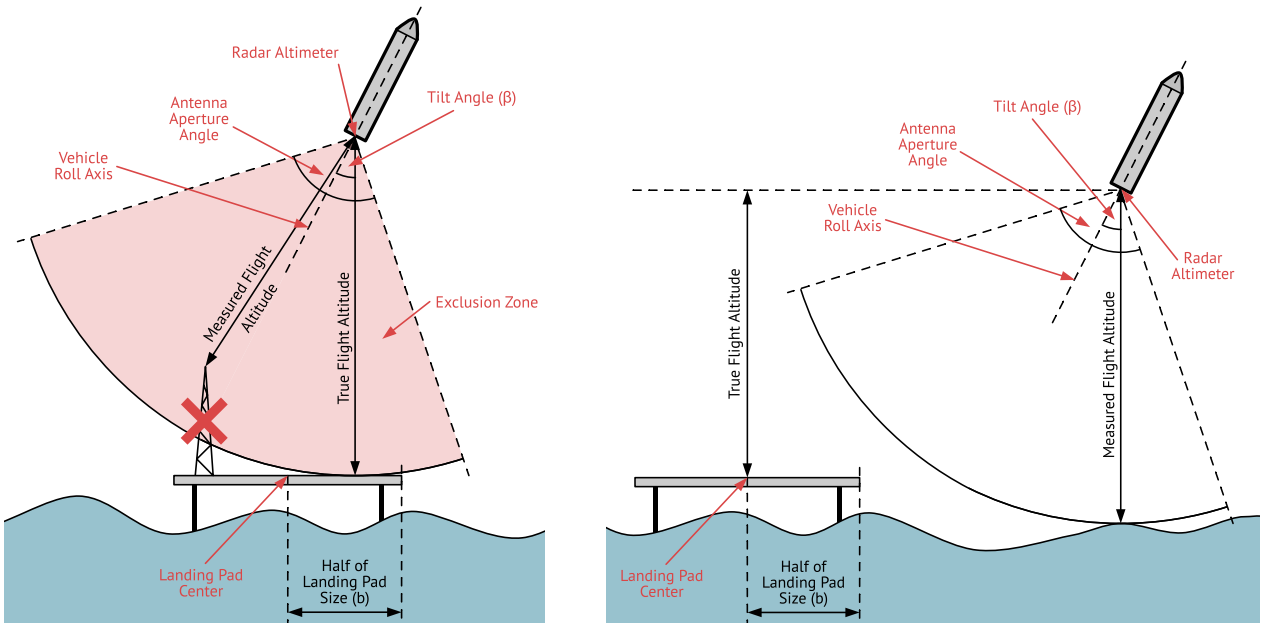

Figure 12: Schematic drawing of the simple radar altimeter measurement principle based on the nearest detectable object. Left picture: Case in which the vehicle is directly above landing pad. The red circular segment is the exclusion zone for the given true flight altitude, where no other objects must be present. Right picture: Vehicle with horizontal displacement to landing pad — nearest detectable is the water, not the landing platform.

angle is chosen large enough to have the entire landing pad in the antenna FoV, taking the maximum horizontal distance to the landing pad center and the maximum tilt angle of the vehicle into account. This way, also objects higher than the landing pad itself (like the ground installations needed for DGNSS operation) are possible, given that they do not obstruct the view to the radar reflectors. A schematic drawing of this measurement principle is depicted in Figure 13.

Independent of the measurement principle, there is currently no experience with operating radar altimeters in the proximity of or even through the LH2/LOx engine exhaust plume. The engine exhaust plume could interfere with the radar measurements, potentially falsifying them or rendering valid measurements even impossible. A test campaign to collect experimental data of this interaction, if any, during an upcoming engine static firing test with radar altimeter prototypes is currently planned.

Another point to be addressed for the radar altimeters are the operational environmental conditions. As the altimeters will be operated close to the engine exhaust plume, they will be subject to very high temperatures, vibrations, and shocks. A protection and qualification concept still needs to be derived, as available radar sensors are usually not operated in such environments.

4.2.3. Flush Airdata Sensing (FADS) System

The Flush Airdata Sensing (FADS) System is widely used for various flight vehicles in subsonic up to transonic and supersonic speed in order to determine the flight angles and to some extend also for velocity and altitude determination. For a backwards flying rocket, the typical design cannot be used due to the very disturbed and complex flow around the vehicle. To overcome this issue, an unusual approach is under investigation for use in the descent configuration of the CALLISTO flight vehicle. Due to the outer position of the fins on top of the vehicle, the fins are exposed to the less disturbed free stream flow. By measuring the pressure on each side of the fin, the local angle of attack can be evaluated and together with the known angle of incident of the fin the global angle of attack can be determined. Finally, the usage of multiple fins allows the calculation of angle of attack and sideslip. In Figure 14, a sketch of the principle is shown.

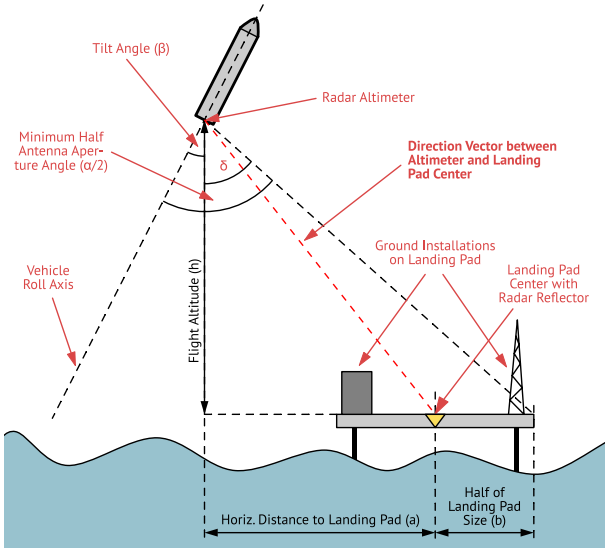

Figure 13: Schematic drawing of the radar altimeter measurement principle.

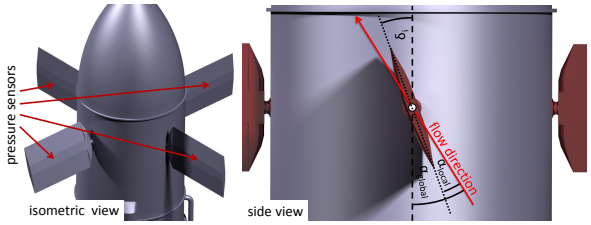

Figure 14: Sketch of the CALLISTO FADS system on fins.

For CALLISTO, the both pairs of fins will be instrumented resulting in redundant measurement in the opposing fin of each pair. The advantage of this concept is — besides the calculation of the flight parameters — a measurement of additional data to determine the health status of the fins during and post flight. Nevertheless, due to the preliminary design phase of CALLISTO, it has to be emphasized that the design is still under investigation especially due to sensor integration issues and shock-boundary layer interactions. An analysis of the achievable system performance is pending as well and might result in changes of the FADS system design.

5. Navigation Performance

5.1. CALLISTO

The performance of the HNS has been assessed by means of simulation of a preliminary version of the Kalman filer which will run aboard the vehicle. Two trajectories, referred to as *Return-to-Launch-Site (RTLS)* and *Downrange (DR)*, have been designed by JAXA and DLR to fit the Test and Demo Flight scenarios, respectively. Figure 15 shows a comparison of the downrange-altitude profiles of the two trajectories. For a matter of brevity, the navigation performance analysis results are shown here for the DR trajectory only, which was chosen because of the — from navigation perspective — more challenging flight envelope, including larger velocity, acceleration, and attitude changes.

The time histories of some trajectory parameters are given in Figure 16 for the DR scenario. In the bottom plot, showing the pitch rate profile, one can see the rotation maneuver taking place before and during the re-entry burn, visible in the specific acceleration plot. This trajectory differs from the one used for previous analyses, such as the one presented in [30], in that it features a larger attitude maneuver during the boost-back phase in order to better address mission objectives.

The second major difference with respect to the previous work is the GNSS receiver model. The results presented here are based on a realistic DGNSS performance model, rather than a simplified Single Point Positioning (SPP) performance model as was the case in [30]. The DGNSS solution is assumed to be available throughout the entire trajectory, whereas radar altimeter measurements become available below 500 m altitude. Additionally, to produce the plots shown in Figure 17, the attitude of the navigation frame with respect to the World Geodetic System 1984 (WGS84) reference at lift-off (i. e., at $t = 0\,\mathrm{s}$) is assumed to be perfectly known. The results shown in the plots of Figure 17 should therefore be considered as the HNS "internal" performance, isolated from initial attitude errors, external mounting errors or vehicle structure misalignments with respect to the WGS84 reference.

The time histories of the 99 % confidence bounds ($\approx 2.57\sigma$) for position, velocity, and attitude error are reported in Figure 17 for the scenario described above. In the top plot, one can see that the vertical position error is larger than the horizontal one during most of the flight, as is expected based on typical GNSS Dilution of Precision (DOP) values, but rapidly decreases towards the end of the flight as radar altimeter fixes become available. This does not show in the velocity plot, as the measurement error was assumed to be isotropic. Additionally, as external forces mainly act along the vehicle's longitudinal axis, the components of the IMU parameters producing errors along this direction are better observable and, therefore, more accurately estimated. These factors lead to an overall better velocity estimate in the vertical direction. Finally, the bottom plot shows a rapid increase in attitude error around the roll axis during the ascent phase due to its limited observability. The magnitude of this error

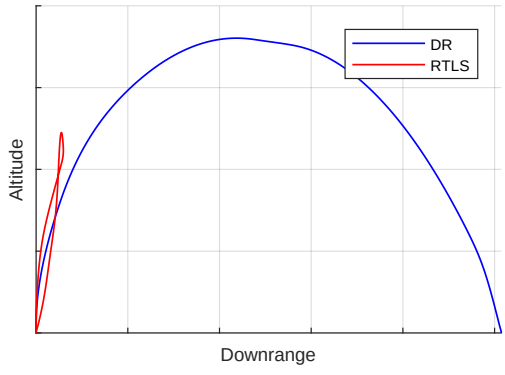

Figure 15: Downrange-altitude profiles comparison for the current DLR/JAXA CALLISTO RTLS/DR trajectories.

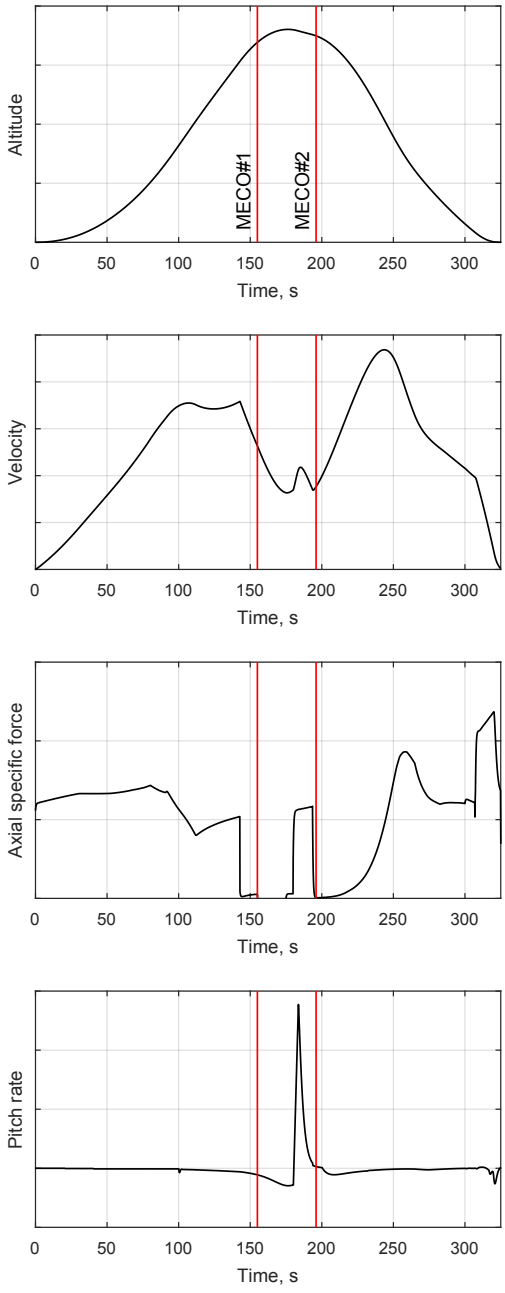

Figure 16: Qualitative evolution of the CALLISTO DR trajectory parameters.

growth mainly depends on IMU uncalibrated parameters and the magnitude of the attitude changes occurring during the ballistic phase, and it is therefore strongly dependent on trajectory design. During the ballistic phase, the attitude change combined with the lack of observability produce further uncertainty growth, affecting most significantly the pitch and yaw components. Finally, during the re-entry burn, the presence of non-inertial accelerations in combination with the GNSS updates make attitude observable, thus causing the decrease in uncertainty visible in the plot.

Of course, in a real case scenario, the attitude of the navigation frame with respect to the WGS84 reference is not perfectly known before launch. Gyro compassing can be performed during the time preceding lift-off to get an initial estimate of such quantity, as well as to improve the accuracy of the estimate of some IMU parameters, such as bias and scale factor. The extent to which attitude can be estimated before launch by means of this procedure has not been analyzed in detail yet. An accurate prediction of the overall attitude accuracy can thus not be made. However, Table 2 shows expected values that are deemed achievable during different flight phases. The Main Engine Cut-Off (MECO) events with respect to which these phases are defined are identified in Figure 16 by the vertical red lines. It should be kept in mind that these quantities are trajectory-dependent and that the values presented here refer to the flight profile currently under consideration.

Phase		**Pitch/Yaw**	**Roll**
From	*To*	[deg]	[deg]
Launch	MECO#1	0.5	2.5
MECO#1	MECO#2	1	1.5
MECO#2	Landing	0.5	0.5

Table 2: Expected achievable attitude accuracy for different flight phases of CALLISTO at 99 % probability.

5.2. *ReFEx*

The navigation performance attainable by the HNS for ReFEx was assessed through covariance analysis that provides a floor for the achievable filter state covariance (see, e. g., [31]). This covariance measure is initialized and propagated along the nominal mission trajectory. At appropriate epochs it is updated with statistical models of the measurements, emulating the sensor fusion algorithm within the HNS. The current analysis uses the most current sensor set and an up-to-date mission trajectory which includes a bank-angle reversal (belly-up to belly-down) maneuver during the descent. In addition, it uses a higher fidelity model of the Sun sensors, accounting for their configuration within the vehicle and their FoV.

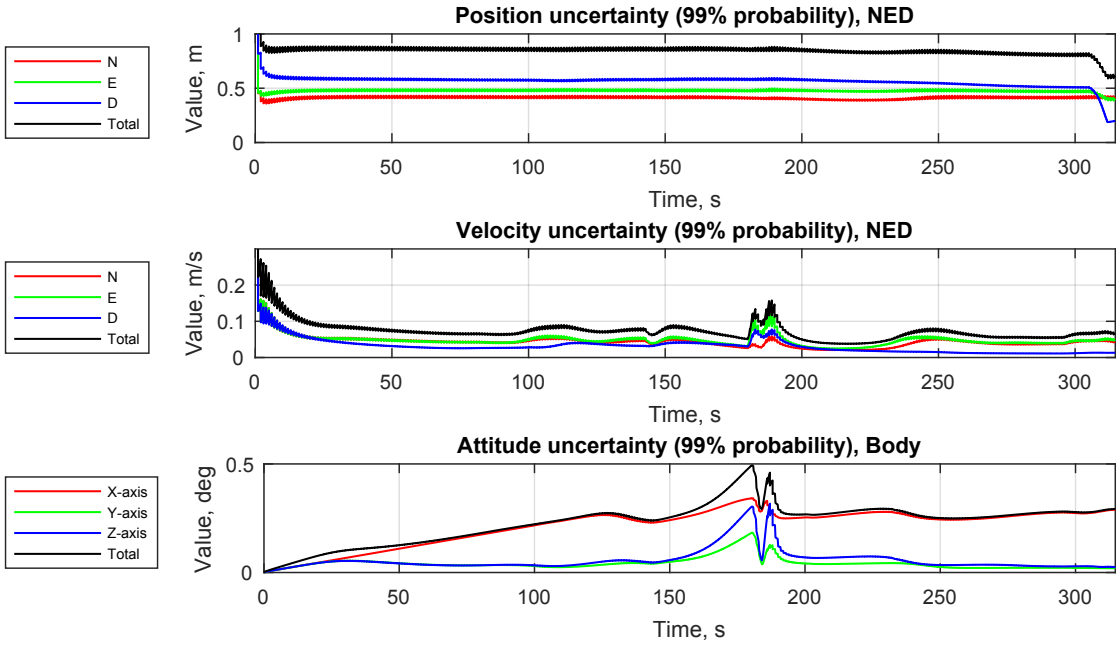

Figure 17: CALLISTO navigation solution error covariance.

5.2.1. Trajectory

The altitude, velocity, linear acceleration, and angular rate profiles of the trajectory followed are shown in Figure 18, where the time origin is the lift-off instant. The mission is split into two phases: a passively stabilized ascent and a controlled descent. During the ascent, the vehicle spins up to 900 °/s for about 80 s, being propelled by two engine burns (one per rocket stage), as is visible in Figure 18; during the descent, the atmospheric reentry decelerates the vehicle. The mentioned bank-angle reversal maneuver is performed during this phase (at around $T = 400\,\mathrm{s}$).

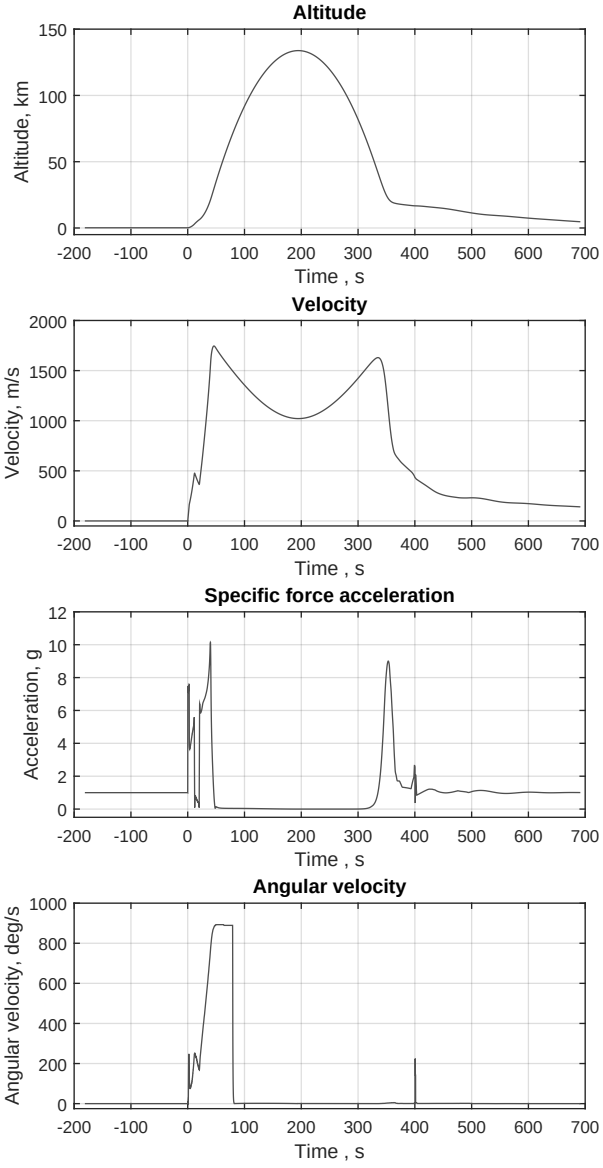

Figure 18: Altitude, total velocity, total specific-force (non-gravitational) acceleration, and angular rate profiles for ReFEx; lift-off at $T = 0\,\mathrm{s}$.

5.2.2. Covariance Results

The results of the filter covariance analysis are displayed in Figure 19 for the HNS with and without Sun sensor aiding, with plots showing position, velocity, and attitude (2-norm) estimation errors (1σ). The initial condition (1σ) is 10 m (all Earth-Centered Earth-Fixed (ECEF) axes), 0.01 m/s (static vehicle in all ECEF directions), and 1° (all body axes). The structure of the IMU filter model used is identical to that in [32] and includes gyroscope and accelerometer bias (turn-on and drift), scale-factor (turn-on and drift), angular/velocity random walk, misalignment, and G-sensitivity (gyroscope only). GPS position and velocity information updates the filter state covariance, emulating the raw GPS measurement inputs in the actual implementation of the HNS. The Sun sensor model includes the field-of-view amplitude and measurement noise. An alignment period of 180 s on the launch pad is simulated through the use of static updates (null velocity and null rate, both with respect to ECEF). As had been observed in [32], the position estimation ac-

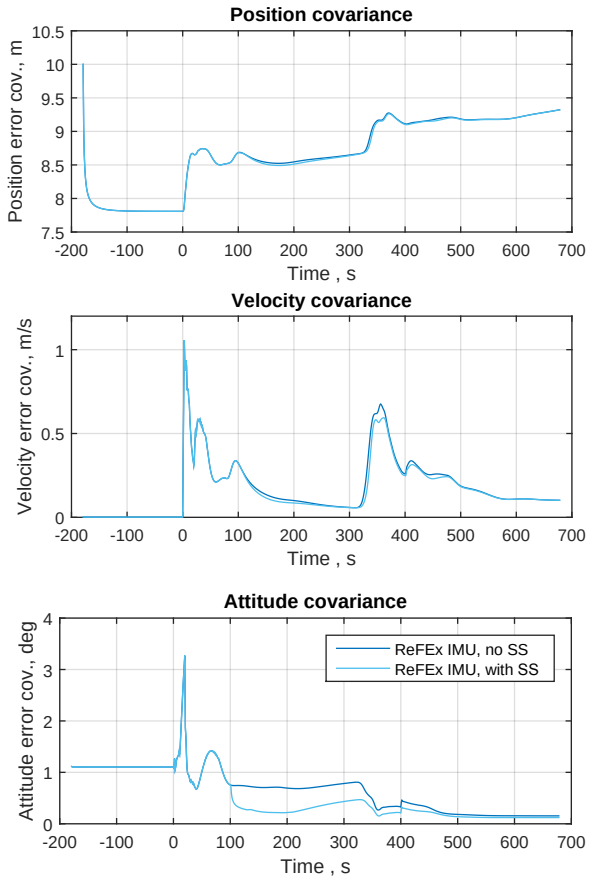

Figure 19: Kinematic state estimation error covariance (1σ) for the ReFEx HNS with or without Sun sensors.

curacy is driven mainly by the GNSS signal quality, i. e., 8 – 10 m (1σ) during flight. Velocity and attitude errors, on the other hand, have a higher dependence on the IMU error model, with the latter being very sensitive to gyroscope performance. Velocity estimation is worse during engine burns and reentry deceleration phase (cf. Figure 18) reaching around 0.5 m/s (1σ); in contrast, steady-state accuracy lies below 0.3 m/s (1σ). As expected, and as also seen in [32], when available, the Sun sensors considerably improve attitude estimation (from about 0.8° to about 0.3° (1σ), within $T \in [102,\ 210]$ s). Velocity and position see only a negligible benefit. At lower altitudes in the descent, when the Sun sensors no longer operate due to atmosphere, the improvement in attitude estimation is gradually lost as the error in this state slowly tends to that of the HNS without Sun sensors.

6. Conclusions and Outlook

The preliminary design of the Hybrid Navigation Systems (HNS) developed for the CALLISTO and ReFEx projects has been presented in detail. The requirements derived from the previous studies and set by both projects in terms of navigation turned out to be challenging. In order to satisfy these requirements, innovative approaches like the DGNSS concept, Sun sensors, radar altimeter systems, and FADS systems, which have not been applied to European launchers before, have been introduced into the HNS sensor suites. While the core building blocks are the same for both HNSs, they deviate in terms of their chosen sensor suites; the commonalities and differences have been outlined. Preliminary performance analyses with the currently selected sensor suites have allowed verification of the compliance with most of the navigation performance requirements under nominal conditions, as well as for some failure scenarios.

However, as the developments are still in a conceptual phase for both projects, the design might still change in the course of the further development.

Future work includes the detailed modeling of the navigation algorithms and a thorough performance analysis using full 6-Degrees of Freedom (DoF) closed-loop simulations combined with the G&C functions for both projects as well as the further development on hardware and software side. This also includes the characterization and verification of the partially and fully assembled HNSs in specialized testing facilities and the setup of a HiL test bench using real-time simulation platforms.

Acknowledgements

The work described in this paper has been funded internally by the German Aerospace Center (DLR), Program Directorate Space Research and Technology, as part of the ongoing projects *Reusability Flight Experiment (ReFEx)* and *Cooperative Action Leading to Launcher Innovation for Stage Tossback Operation (CALLISTO)*, whereas CALLISTO is a trilateral project with joint research activities of the French National Center for Space Studies (CNES), DLR, and the Japan Aerospace Exploration Agency (JAXA). The authors gratefully acknowledge the collaboration with CNES and JAXA and the valuable discussions with all members of the CALLISTO and ReFEx project teams and other colleagues across all DLR sites.

References

[1] Stephan Theil, Markus Schlotterer, Marcus Hallmann, Michael Conradt, Markus Markgraf, and Inge Vanschoenbeek. Hybrid Navigation System for the SHEFEX-2 Mission. In *AIAA Guidance, Navigation and Control Conference and Exhibit*, Honolulu, Hawaii, USA, August 18–21, 2008. AIAA Paper No. 2008-6991.

[2] Stephan Theil, Markus Schlotterer, Michael Conradt, and Marcus Hallmann. Integrated Navigation System for the second SHarp Edge Flight EXperiment (SHEFEX-2). In *Proceedings of the 31th Annual AAS Guidance and Control Conference*, Breckenridge, Colorado, USA, February 1–6, 2008. AAS Paper No. 08-012.

[3] Stephan Theil, Stephen Steffes, Malak Samaan, Michael Conradt, Markus Markgraf, and Inge Vanschoenbeek. Hybrid Navigation System for Spaceplanes, Launch and Re-Entry Vehicles. In *16th AIAA/DLR/DGLR International Space Planes and Hypersonic Systems and Technologies Conference*. AIAA, October 2009.

[4] René Schwarz and Stephan Theil. A Fault-Tolerant On-Board Computing and Data Handling Architecture Incorporating a Concept for Failure Detection, Isolation, and Recovery for the SHEFEX III Navigation System. In *Proceedings of the 13th International Conference on Space Operations (SpaceOps), May 5–9, 2014, Pasadena, California*. American Institute of Aeronautics and Astronautics (AIAA), May 8, 2014. AIAA Paper No. 2014-1874.

[5] Stephen Steffes, Stephan Theil, Malak A. Samaan, and Michael Conradt. Flight Results from the SHEFEX2 Hybrid Navigation System Experiment. In *2012 AIAA Guidance, Navigation, and Control Conference*, Minneapolis, Minnesota, USA, August 13–16, 2012. AIAA Paper No. 2012-4991.

[6] Stephen Steffes. Real-Time Navigation Algorithm for the SHEFEX2 Hybrid Navigation System Experiment. In *2012 AIAA Guidance, Navigation, and Control Conference*, Minneapolis, Minnesota, USA, August 13–16, 2012. AIAA Paper No. 2012-4990.

[7] Malak Samaan and Stephan Theil. Development of a Hybrid Navigation System for the Third Sharp Edge Flight Experiment (SHEFEX-3). In *2013 AAS/AIAA Astrodynamics Specialist Conference*, Hilton Head Island, South Carolina, USA, August 11–15, 2013. AAS Paper No. 13-877.

[8] Stephen R. Steffes. *Development and Analysis of SHEFEX-2 Hybrid Navigation System Experiment*. PhD thesis, University of Bremen, April 2013.

[9] Shinji Ishimoto, Pascal Tatiossian, and Etienne Dumont. Overview of the CALLISTO Project. In *32nd Internationational Symposium on Space Technology and Science (ISTS). June 15–21, 2019, Fukui, Japan*, 2019.

[10] Etienne Dumont, Shinji Ishimoto, Pascal Tatiossian, Josef Klevanski, Bodo Reimann, Tobias Ecker, Lars Witte, Johannes Riehmer, Marco Sagliano, Sofia Giagkozoglou-Vincenzino, Ivaylo Petkov, Waldemar Rotärmel, René Schwarz, David Seelbinder, Markus Markgraf, Jan Sommer, Dennis Pfau, and Hauke Martens. CALLISTO: a Demonstrator for Reusable Launcher Key Technologies. In *32nd Internationational Symposium on Space Technology and Science (ISTS). June 15–21, 2019, Fukui, Japan*, 2019.

[11] Martin Sippel, Chiara Manfletti, and Holger Burkhardt. Long-term/strategic scenario for reusable booster stages. *Acta Astronautica*, 58(4):209 – 221, 2006.

[12] François Deneu. *Selection and Design Process of TSTO Configurations*.

[13] Peter Rickmers and Waldemar Bauer. ReFEx: Reusability Flight Experiment – A Project Overview. In *8th European Conference for Aeronautics and Space Sciences (EUCASS), Conference on "Reusable Systems for Space Access". July 1–4, 2019, Madrid, Spain*. EUCASS association, 2019.

[14] Lars Johannsen. Erarbeitung eines Konzeptes zur aktiven Steuerung einer hochzuverlässigen Leistungsversorgungseinheit für ein hybrides Navigationssystem. Bachelor's, Hochschule Bremen, July 2015.

[15] Norbert Kwiatkowski. Entwicklung eines Referenzdesigns einer hochverfügbaren Leistungsversorgungseinheit für das Shefex III- Navigationssystem. Bachelor's, Hochschule Wilhelmshaven, January 2014.

[16] Norbert Kwiatkowski. Entwicklung von Test- und Verifikationsprozeduren für eine hochverfügbare Leistungsversorgungseinheit auf Basis einer Fehlermöglichkeits- und -einflussanalyse. Master's thesis, Hochschule Wilhelmshaven, December 2015.

[17] Samy Ayoub. Development of a Power Distribution Unit Controller for the SHEFEX III Navigation System. Master's thesis, Cologne University of Applied Sciences, July 2015.

[18] Martin Reigenborn. Development and Verification of a Power Distribution Unit Controller Software for a Hybrid Navigation System. Master's thesis, Technische Universität Berlin, October 2018.

[19] Real-Time Executive for Multiprocessor Systems. http://www.rtems.org. Accessed: 2019-06-11.

[20] Alexander Krutwig AK and Sebastian Huber SH. RTEMS SMP Status Report. 2015.

[21] OUTPOST - Open modUlar sofTware PlatfOrm for SpacecrafT. http://github.com/DLR-RY/outpost-core. Accessed: 2019-06-11.

[22] Zain A. H. Hammadeh, Tobias Franz, Olaf Maibaum, Andreas Gerndt, and Daniel Lüdtke. Event-Driven Multithreading Execution Platform for Real-Time On-Board Software Systems. In *Operating Systems Platforms for Embedded Real-Time applications (OSPERT)*, July 2019. to appear.

[23] Olaf Maibaum and Ansgar Heidecker. Software Evolution from TET-1 to Eu: CROPIS. In *10th IAA International Symposium on Small Satellites for Earth Observation*, 2015.

[24] Oliver Montenbruck, Eberhard Gill, and Markus Markgraf. Phoenix-XNS-a miniature real-time navigation system for LEO satellites. In *3rd ESA Workshop on Satellite Navigation User Equipment Technologies, NAVITEC*, pages 11–13, 2006.

[25] Markus Markgraf and Oliver Montenbruck. Phoenix-HD—a miniature GPS tracking system for scientific and commercial rocket launches. In *6th International Symposium on Launcher Technologies*, 2005.

[26] Sigtec Navigation Pty Ltd. *"MG5000 Series User Guide"; MG5-200-GUIDS-User Guide*, August 2003. Issue B-T08.

[27] Stephen A. Whitmore, Brent R. Cobleigh, and Edward A. Haering. Design and Calibration of the X-33 Flush Airdata Sensing (FADS) System. Technical Memorandum NASA/TM-1998-206540, NASA Dryden Flight Research Center, January 1998. Presented at the AIAA Aerospace Sciences Meeting and Exhibit, January 12–15, 1998, Reno, Nevada. AIAA-98-0201.

[28] André Hauschild, Markus Markgraf, Oliver Montenbruck, Horst Pfeuffer, Elie Dawidowicz, Badr Rmili, and Alain Conde Reis. Results of the GNSS receiver experiment OCAM-G on Ariane-5 flight VA 219. *Proceedings of the Institution of Mechanical Engineers Part G-Journal of Aerospace Engineering*, 231(6):1100–1114, 2016.

[29] Waldemar Kunysz et al. High Performance GPS Pinwheel Antenna. In *Proceedings of the 2000 international technical meeting of the satellite division of the institute of navigation (ION GPS 2000)*, page 19–22, 2000.

[30] René Schwarz, Marco Solari, Bronislovas Razgus, Michael Dumke, Markus Markgraf, Matias Bestard Körner, Dennis Pfau, Martin Reigenborn, Benjamin Braun, and Jan Sommer. Preliminary Design of the Hybrid Navigation System (HNS) for the CALLISTO RLV Demonstrator. In *8th European Conference for Aeronautics and Space Sciences (EUCASS)*, Juli 2019.

[31] Niclas Bergman. *Recursive Bayesian Estimation: Navigation and Tracking Applications*. PhD thesis, Linköping University, Sweden, 1999.

[32] M. Sagliano, G. F. Trigo, and R. Schwarz. Preliminary Guidance and Navigation Design for the Upcoming DLR Reusability Flight Experiment (ReFEx). In *69th International Astronautical Congress*, Bremen, Germany, 2018.